Information processing with unstable memories

J. J. Torres*, J. M. Cortés† and J. Marro*

*Institute Carlos I for Theoretical and Computational Physics, University of Granada, Fuentenueva s/n E-18071 Granada, Spain
†Institute for Adaptive and Neural Computation, School of Informatics, University of Edinburgh, 5 Forrest Hill, EH1 2QL, UK.

Abstract. We present a theoretical framework which allows one to study both theoretically and numerically the effect of including activity dependent mechanisms in the dynamics of synapses in simple neural networks. In particular, we study synaptic changes at different time scales from less than the millisecond (fast synaptic noise) to the scale of learning (say years). For some limits of interest, as a consequence of such dynamics, the fixed-point solutions or attractors loose stability and the system shows enhancement of his response to changing external stimuli. In some conditions, this results in a novel phase in which the neural activity continously jumps among different activity patterns.

Keywords: Synaptic depression, synaptic facilitation, dynamical memories, attractor neural networks
PACS: 05.10.-a, 84.35.+i, 87.19.La

INTRODUCTION AND BASIC MODEL

In the last decade or so, synapses have been shown to be more than simple communication lines, namely, it has been extensively reported that many dynamical processes taking place in the synapses can influence and even determine the transmission of information [1]. The relevant mechanisms can occur at different time scales. In the long time, synapses modify their intensity as a consequence of learning, which occurs in a time scale higher than the second, say days or even years. This is now demonstrated both in vivo and in vitro experiments, and it has received wide theoretical attention, e.g., the theory of learning in attractor neural networks [2, 3]. On the other hand, it has been described that fast synaptic fluctuations coupled with other mechanisms during the transmission of information could determine a large variety of computations in the brain [4, 5]. These fluctuations occur at very short (less than the millisecond) temporal scales, and they seem to have different causes. For instance, the stochasticity of the opening and closing of the neurotransmitter vesicles, the stochasticity of the postsynaptic receptor, which in turn has several sources, e. g., variations of the glutamate concentration in the synaptic cleft, and differences in the power released from different locations on the active zone of the synapses [6]. Finally, it has also been reported that actual synapses endure activity-dependent mechanisms, such as short-time depression and/or facilitation, which occur in the temporal scale of neural activity. That is, it seems that periods of elevated presynaptic activity may cause either decrease or increase of the neurotransmitter release and, consequently, that the postsynaptic response is either depressed or facilitated depending on the presynaptic neural activity [1, 7, 8]. This has been reported

CP887, *Cooperative Behavior in Neural Systems: Ninth Granada Lectures*
edited by J. Marro, P. L. Garrido, and J. J. Torres

to be necessary to produce a noticeable synaptic plasticity [1], which is fundamental for the development and adaptation of the nervous system, and it is also believed to be the basis for higher functions such as learning and memory.

In spite of this rather clear-cut picture, which is been extracted from set of data whose amount and quality is rapidly increasing these days, a general theory is lacking. That is, the result of many neurons cooperating through synapses that undergo all these types of mechanisms, which may compete with each other and with other possible variables, is not fully understood yet. In particular, of special interest is to understand how these synaptic mechanisms affect the fixed points of the neural activity and their stability, which concerns memory and recall processes. In this paper we present an attempt towards a theoretical framework to study the influence of synaptic changes on the collective properties of different types of neural circuits.

Let us consider a set of N (binary, for simplicity [9]) neurons with configurations $\mathbf{S} \equiv \{s_i = \pm 1; i = 1, \ldots, N\}$ connected by synapses of intensity

$$w_{ij} = \overline{w}_{ij} x_j \ \ \forall i, j. \tag{1}$$

Here, $\overline{w}_{ij} = 1/N \sum_{\mu=1}^{M} \Xi_i^\mu \Xi_j^\mu$ are fixed and determined in a previous slow *learning* process in which the network stores M patterns of neural activity, $\Xi^\mu \equiv \{\Xi_i^\mu = \pm 1; i = 1, \ldots, N\}$ ($\mu = 1 \ldots M$). The weights $\overline{w}_{ij}$ represent maximal averaged synaptic conductances between the presynaptic neuron j and the postsynaptic neuron i, while, $x_j \in \mathbb{R}$ is a stochastic variable that influences these maximal conductances and takes into account other synaptic dynamics than those due to long-time learning. For fixed $\mathbf{W} \equiv \{\overline{w}_{ij}\}$, the network state at time t is determined by $\mathbf{A} = (\mathbf{S}, \mathbf{X} \equiv \{x_i\})$. This evolves in time according to

$$\frac{\partial P_t(\mathbf{A})}{\partial t} = \sum_{\mathbf{A}'} \left[P_t(\mathbf{A}') c(\mathbf{A}' \to \mathbf{A}) - P_t(\mathbf{A}) c(\mathbf{A} \to \mathbf{A}') \right] \tag{2}$$

where $c(\mathbf{A} \to \mathbf{A}') = p\, c^{\mathbf{X}}(\mathbf{S} \to \mathbf{S}')\, \delta_{\mathbf{X},\mathbf{X}'} + (1-p)\, c^{\mathbf{S}}(\mathbf{X} \to \mathbf{X}')\, \delta_{\mathbf{S},\mathbf{S}'}$ [11]. This amounts to assume that neurons ($\mathbf{S}$) change stochastically in time competing with a noisy dynamics of synapses ($\mathbf{X}$), the latter with an *a priory* relative weight of $(1-p)/p$.

For $p = 1$, the model reduces to the Hopfield case, in which synapses are quenched, i.e., x_i is constant and independent of i. Without loosing any generality we can assume $x = 1$. This limit has been widely studied in the last decades and it is beyond the scope of the present work. In the next sections we study the more interesting case of $p \to 0$, which describes fast synaptic fluctuations. Afterwards we shall study a particular example of the general case $p < 1$, which assumes a coupled dynamics for neurons and synapses in the same temporal scale.

THE LIMIT OF FAST FLUCTUATIONS AND THE EMERGENCE OF UNSTABLE MEMORIES

The limit of $p \to 0$ describes fast synaptic noise affecting the synapses, which can have different causes as mentioned above. Recordings in real experiments show that these fluctuations are very fast – of order of the millisecond – compared with the typical mean inter-spike interval. We can then use in Eq. (2) the limit $p \to 0$ to take into account these

fluctuations. In this limit, one can uncouple the stochastic dynamics for neurons ($\mathbf{S}$) and the synaptic noise ($\mathbf{X}$) using standard techniques [12]. It follows that neurons evolve as in the presence of a steady distribution for the noise $\mathbf{X}$: If we write $P_t(\mathbf{A}) = P_t(\mathbf{X}|\mathbf{S})P_t(\mathbf{S})$, where $P_t(\mathbf{X}|\mathbf{S})$ stands for the conditional probability of $\mathbf{X}$ given $\mathbf{S}$, one obtains from (2), after rescaling time $tp \to t$ and summing over $\mathbf{X}$, that

$$\frac{\partial P_t(\mathbf{S})}{\partial t} = \sum_{\mathbf{S}'} \left\{ P_t(\mathbf{S}')\bar{c}[\mathbf{S}' \to \mathbf{S}] - P_t(\mathbf{S})\bar{c}[\mathbf{S} \to \mathbf{S}'] \right\}. \tag{3}$$

Here, $\bar{c}[\mathbf{S} \to \mathbf{S}'] \equiv \sum_{\mathbf{X}} P^{\rm st}(\mathbf{X}|\mathbf{S})\, c^{\mathbf{X}}[\mathbf{S} \to \mathbf{S}']$, and the stationary distribution for the noise is

$$P^{\rm st}(\mathbf{X}|\mathbf{S}) = \frac{\sum_{\mathbf{X}} c^{\mathbf{S}}[\mathbf{X}' \to \mathbf{X}]\, P^{\rm st}(\mathbf{X}'|\mathbf{S})}{\sum_{\mathbf{X}} c^{\mathbf{S}}[\mathbf{X} \to \mathbf{X}']}. \tag{4}$$

The expression (4) involves an assumption on how synaptic noise depends on the overall neural activity. An interesting specific situation is to assume activity-dependent synaptic *noise* consistent with short-term synaptic depression and/or facilitation [7, 10]. That is, let us assume that $P^{\rm st}(\mathbf{X}|\mathbf{S}) = \prod_j P(x_j|\mathbf{S})$ with

$$P(x_j|\mathbf{S}) = \zeta(\vec{\mathbf{m}})\ \delta(x_j - \Phi) + [1 - \zeta(\vec{\mathbf{m}})]\ \delta(x_j - 1). \tag{5}$$

Here, $\vec{\mathbf{m}} = \vec{\mathbf{m}}(\mathbf{S}) \equiv \left(m^1(\mathbf{S}), \ldots, m^M(\mathbf{S})\right)$ is the M-dimensional overlap vector, and $\zeta(\vec{\mathbf{m}})$ stands for a function of $\vec{\mathbf{m}}$ to be determined. With this choice, the average over the distribution (5) of the noise variable is $\overline{x_j} \equiv \int x_j P(x_j|\mathbf{S}) dx_j = 1 - (1-\Phi)\zeta(\vec{\mathbf{m}})$ and the variance is $\sigma_x^2 = (1-\Phi)^2 \zeta(\vec{\mathbf{m}})[1 - \zeta(\vec{\mathbf{m}})]$. Note that these two quantities depend on time for $\Phi \neq 1$ through the overlap vector $\vec{\mathbf{m}}$, which is a measure of the activity of the network. Moreover, the depression/facilitation effect in (5), namely $x_j = \Phi > 0$ ($\Phi \neq 1$), depends through the probability $\zeta(\vec{\mathbf{m}})$ on the overlap vector, which is related to the net current arriving to postsynaptic neurons. Consequently, the non–local choice (5) introduces non–trivial correlations between synaptic noise and neural activity. One has a depressing (facilitating) effect for $\Phi < (>)1$, and the trivial case $\Phi = 1$ corresponds to the static Hopfield model with static synapses. Note that, although the fast noise dynamics occurs at a very small time scale, the depressing or facilitating mechanism occurs at the time scale of the neural activity –via the coupling with the overlap vector through the function $\zeta(\vec{\mathbf{m}})$.

The interest is on the nature of the fixed point solutions of Eqs. (3-5) and their stability. This can be done in the case of asynchronous *sequential spin–flip* dynamics for the neurons, namely, stochastic local inversions $s_i \to -s_i$ as induced by a bath at temperature T. The elementary rate then reduces to $c^{\mathbf{X}}[\mathbf{S} \to \mathbf{S}'] = \Psi[u^{\mathbf{X}}(\mathbf{S}, i)]$, where we assume $\Psi(u) = \exp(-u)\Psi(-u)$, $\Psi(0) = 1$, $\Psi(\infty) = 0$ and $u^{\mathbf{X}}(\mathbf{S}, i) \equiv 2T^{-1} s_i h_i^{\mathbf{X}}(\mathbf{S})$ [12]. Here $h_i^{\mathbf{X}}(\mathbf{S}) = \sum_{j \neq i} w_{ij} x_j s_j$ is the net presynaptic current or local field on the (postsynaptic) neuron i. In the following we use $\Psi(u) = e^{-u/2}$. Under the standard mean field assumption $s_i = \langle s_i \rangle$, the simplest situation occurs for only one stored pattern, that is $M = 1$. In this case, one easily obtains the mean-field fixed-point equation (See [13] for details),

$$m = \tanh\left\{ T^{-1} m \left[1 - (m)^2 (1 - \Phi) \right] \right\}, \tag{6}$$

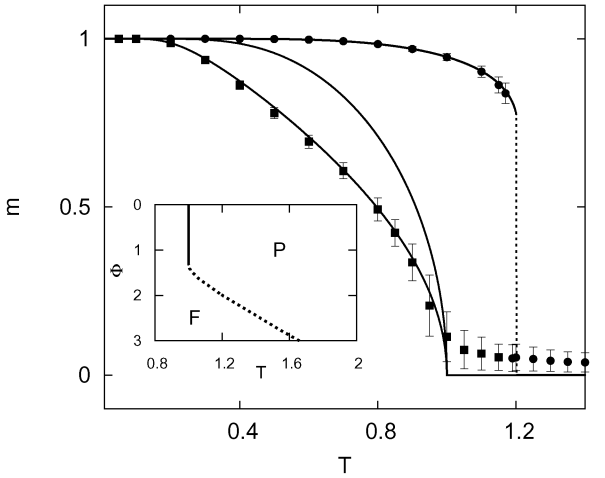

FIGURE 1. Stable steady-state memory solutions of the map (6) as a function of T and from bottom to top, $\Phi = 0.5, 1, 2$ corresponding to depression, static and facilitation situations, respectively. Data points correspond to Monte Carlo simulations for $\Phi = 0.5, 2$ showing the accuracy of the mean field results. The graph in the inset is the phase diagram (T, Φ), where second (solid) and first (dashed) order transition between the memory (F) and non-memory (P) phases are depicted.

$m \equiv m^{\nu=1}$, which preserves the symmetry ± 1. Local stability of the solutions requires that

$$|m| > m_c(T) = \frac{1}{\sqrt{3}} \left(\frac{T_c - T}{\Phi_c - \Phi} \right)^{\frac{1}{2}}. \tag{7}$$

The behavior of (6) is illustrated in Fig. 1 for several values of Φ. This indicates a transition from a *ferromagnetic–like* phase, i.e., solutions $m \neq 0$ with associative memory, to a *paramagnetic–like* phase, $m = 0$. The transition is continuous or second order only for $\Phi < \Phi_c = 4/3$, and it then follows a critical temperature $T_c = 1$. The inset of Fig. 1 shows the tricritical point at (T_c, Φ_c) and the general dependence of the transition temperature with Φ. This result differs dramatically from the standard Hopfield fixed point solutions. For a given temperature, the effect of fast synaptic noise is to decrease the net current arriving to the postsynaptic neuron (which is proportional to the overlap m) for $\Phi < 1$, as in actual depressing synapses, and to increase it for $\Phi > 1$, as in the case of facilitating synapses. Moreover, an additional effect is the increase of the sensitivity of the network response when an external stimulus is applied in the case of depressing fast noise ($\Phi < 1$), see Fig. 2.

This inherent instability of the attractors becomes even more clear when one uses a different type of neuron updating running from asynchronous sequential to totally synchronous parallel updating (see Ref. [14] for a detailed study) resulting in the appearance of a oscillatory phase in which the neural activity continously jumps among the stored

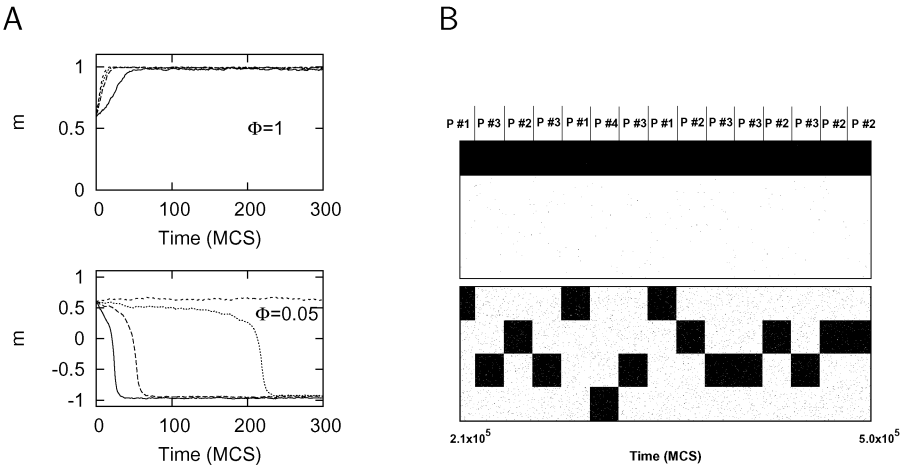

FIGURE 2. Sensitivity of a neural network under external stimulation in the presence of noise induced synaptic depression: Panel A shows, for a single stored pattern, the effect of a weak external stimulus $I^{\text{ext}} = -\delta\xi$ with $\delta \ll 1$. This stimulus tries to drive the activity of the network from the basin of attraction of the pattern towards the antipattern. The top graph corresponds to the case of static classical synapses ($\Phi = 1$) and the bottom for the case of noise induced depression ($\Phi = 0.05$). All simulations were performed at temperature $T = 0.15$. Lines in each graph are from above for $\delta = 0.2, 0.25, 0.3, 0.4$. Panel B shows the sensitivity of the system under repetitive external random stimulus when the network stored 4 overlapping patterns. The top graph shows the Hopfield static case ($\Phi = 1$), and the bottom the noise induced depression case with $\Phi = 0.1$. Here, neuron activity is represented at vertical axis, and simulation parameters are $N = 400$, $T = 0.1$ and $\delta = 0.3$

memories or *attractors*. In some conditions, this dynamics become chaotic which allows for a more efficient dynamical retrieval of memories (see Fig. 3). Defining n as the number of neurons that are updated synchronously at the same time step, one can visualize how the dynamical properties of the network change when one increases the density $\rho \equiv n/N$. This is shown in Fig. 3 where we plotted phase trajectories of the mean firing rate defined as $f \equiv \frac{1}{2N}\sum_i (1 + s_i)$. When one increases ρ from 0 to $\rho = 0.443$ in the simulation presented in the figure, the network stable memories become unstable and transitions between nearest memories occur. If one increases ρ even more, dynamical transitions between more distant memories begin to occur, and the time during which the activity of the network is close to a particular memory also decreases (not shown). Finally, if we increase ρ more (for instance, around $\rho = 0.6$ in Fig. 3), there is a transition to a state in which the activity of the network rapidly jumps between a memory pattern and its antipattern.

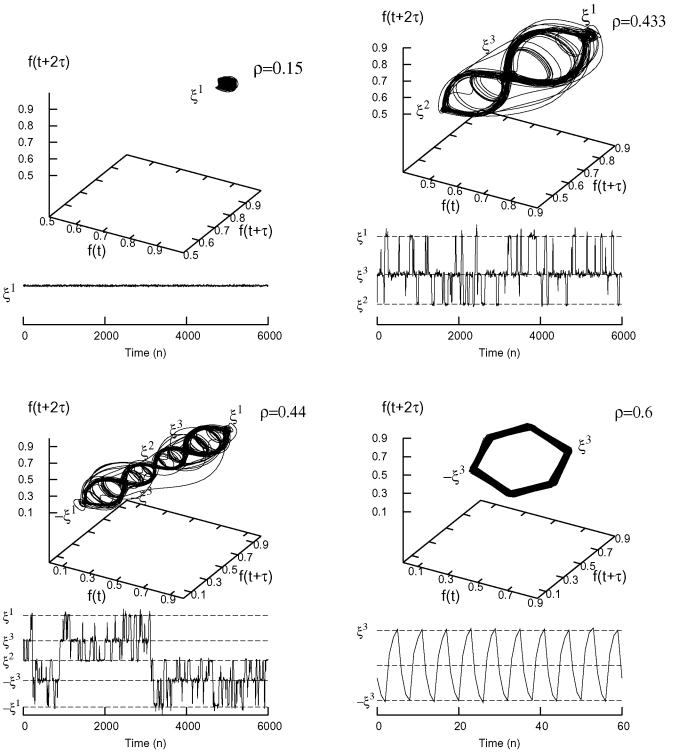

FIGURE 3. Chaotic itineracy in a neural network with depressing fast noise ($\Phi = 0.05$) under the effect of an hybrid updating. The graph shows how by increasing the density of neurons that are being synchronously updated, that is ρ, the number of visited attractors is also increased until a value at which a periodic jumping between a pattern and its antipattern occurs. To build all phase-plane trajectories we used standard false-neighbours techniques with a time delay of $5n$ and an embedding dimension of 5. Simulation parameters are $N = 1600$ and $T = 0.006$.

MODEL OF DYNAMICAL SYNAPSES FOR $p > 0$ AND ITS EFFECT ON MEMORY STABILITY

At intermediate value of p, we may consider synaptic temporal changes in the same scale that the typical interspike interval of neuron activity, that is, in the range of a few milliseconds. This is consistent with actual neural media where activity-dependent mechanisms, such as short-term depression and facilitation, operate at the time scale of neural activity. In this section, we study the interplay between these synaptic mecha-

nisms and the neural activity within a mean-field approach. Our starting point will be now the phenomenological model of dynamical synapses introduced in [7]. We conclude on the implications of a competition between synaptic depression and facilitation on the performance of a neural network.

As above, we consider N binary neurons and use the formalism introduced previously for $p > 0$. The distribution for the synaptic noise is now

$$P(x_j|\mathbf{S}) = \delta[x_j - \Phi_j(t)], \tag{8}$$

which in fact impedes any kind of fast synaptic noise. Here, $\overline{x_j} = \Phi_j(t) \equiv \mathscr{D}_j(t)\,\mathscr{F}_j(t)$, that is, the mean is the product of two dynamical variables that evolve in the time scale of the neural activity, namely t, and represents the state of the dynamical synapse connecting neurons i and j with depressing ($\mathscr{D}_j(t)$) and facilitating ($\mathscr{F}_j(t)$) mechanisms. With the choice (8), the microscopic dynamics describing stochastic neuron changes is $\bar{c}[\mathbf{S} \to \mathbf{S}'] = \Psi[u(\mathbf{S},i)]$, where $u(\mathbf{S},i) \equiv 2T^{-1}s_i h_i(\mathbf{S})$. In the following we will consider the rate $\Psi(u) = 1/2[1 - \tanh(u)]$ which also satisfies the required symmetry and normalization conditions and results most adequate when one considers all the neurons synchronously updated.

Using parallel synchronous updating, each neuron follows the probabilistic dynamics

$$\text{Prob}\{\sigma_i(t+1) = 1\} = \frac{1}{2}\left\{1 + \tanh\left[2T^{-1}h_i(t)\right]\right\}, \tag{9}$$

where $\sigma_i \equiv \frac{1}{2}(1+s_i)$, $\sigma' = \sigma(t+1)$ and we only consider spin-flip changes. The local fields $h_i(t) = \sum_{j=1}^{N} \overline{w}_{ij}\mathscr{D}_j(t)\,\mathscr{F}_j(t)\,\sigma_j(t) - \theta_i$ represents the total presynaptic current arriving to the postsynaptic neuron i. Here, θ_i is the threshold of neuron i to fire. Again, $\overline{w}_{ij}$ are the static synaptic weights due to M stored patterns, namely, $\xi^\nu \equiv \{\xi_i^\nu = 1,0\}, \nu = 1,\ldots,M$. In the present $1,0$ code, it turns out convenient to choose the standard covariance learning rule, namely, $\overline{w}_{ij} = \frac{1}{Na(1-a)}\sum_{\nu=1}^{M}(\xi_i^\nu - a)(\xi_j^\nu - a)$ with $\langle \xi_i^\nu \rangle = a$.

The complete dynamics for depression $\mathscr{D}_j(t)$ and facilitation $\mathscr{F}_j(t)$ was reported in [7]. Here, we use a simplified version of that model in which $\mathscr{D}_j(t) \equiv r_j(t)$ and $\mathscr{F}_j(t) \equiv U + (1-U)u_j(t)$, being $r_j(t)$ the fraction of neurotransmitters which are in a recovered state. A fraction of these neurotransmitters, namely, $Ur(t)$, is ready to be released after the arrival of a presynaptic action potential ($\sigma_j = 1$). The remaining, $(1-U)r(t)$, can also be released by facilitating mechanisms whose dynamics is driven by the variable $u_j(t)$. For simplicity, we assume that the complete dynamics is described by the discrete system of equations

$$\begin{aligned} r_j(t+1) &= r_j(t) + \frac{1 - r_j(t)}{\tau_{\text{rec}}} - U r_j(t)\,\sigma_j(t) - (1-U)\,u_j(t)\,r_j(t)\,\sigma_j(t), \\ u_j(t+1) &= u_j(t) - \frac{u_j(t)}{\tau_{\text{fac}}} + U\left[1 - u_j(t)\right]\sigma_j(t), \end{aligned} \tag{10}$$

where τ_{rec} and τ_{fac} are the time constants for depressing and facilitating mechanisms, respectively. Again, as in the model of the previous section, the static Hopfield case is recovered for $\overline{x_j} = 1$. This can be achieved in the present model for $\tau_{\text{rec}} \to 0$ and $U = 1$.

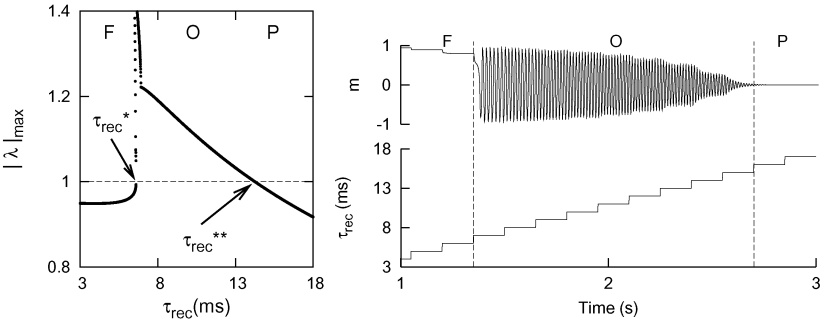

FIGURE 4. (Left) Behaviour of the maximum absolute value for the eigenvalues driving the dynamics around the fixed points, for $U = T = 0.1$ and $\tau_{\text{fac}} = 20$ ms. Here, τ^{*}_{rec} and τ^{**}_{rec} are, respectively, the critical points at which the ferromagnetic (F) and oscillatory phases (O) become unstable. For $\tau_{\text{rec}} > \tau^{**}_{\text{rec}}$, the paramagnetic states (P) are the only ones that remain stable. (Right) The emergence of different dynamical behaviours by continously increasing τ_{rec} from 4 to 18 during 3 seconds.

The system of equations (9-10) can be solved within the standard mean field approach $\sigma_i \approx \langle \sigma_i \rangle$ and in the limit of only one stored pattern $\alpha \equiv M/N = 0$ and $a = 1/2$. Most of our conclusions are also valid for many patterns, however, as we will show latter. The result is a discrete 6-dimensional map, $\vec{y}_{t+1} = \vec{F}(\vec{y}_t)$, where $\vec{y} \equiv \{m_+, m_-, r_+, r_-, u_+, u_-\}$ is a vector whose components are order parameters which measure, respectively, the overlap with the stored pattern ($m = m^1$), the mean depression level (r) and the mean facilitation level (u), in the neurons that are active ($+$) or inactive ($-$) [15]. The local stability of the steady state solutions can be studied by analyzing the behavior of the eigenvalues, namely λ_i associated to the local dynamics of this map (see Ref. [15] for further details). In particular, fixed points become unstable when the maximum absolute value of all eigenvalues, namely, $|\lambda|_{max}$ is bigger than one. Fig. 4(left) shows $|\lambda|_{max}$ as a function of τ_{rec} for $U = T = 0.1$ and $\tau_{\text{fac}} = 20$ ms. Then, the analysis of the stability of fixed points reveals three different regimes in the behaviour of the system. First, a ferromagnetic-like phase associated to standard associative memory appears for $\tau_{\text{rec}} < \tau^{*}_{\text{rec}}$. Second a paramagnetic-like or non-memory phase occurs for $\tau_{\text{rec}} > \tau^{**}_{\text{rec}}$. Finally, an oscillatory phase in which the network activity is jumping between different memories appears for $\tau^{*}_{\text{rec}} < \tau_{\text{rec}} < \tau^{**}_{\text{rec}}$. Fig. 4(right) shows the emergence of these three phases when one continously varies τ_{rec} in the interval $[3, 18]$ during three seconds. Fig. 5 shows phase diagrams obtained by plotting the critical lines at which transitions between these three phases occur for different values of the parameters $\tau_{\text{rec}}, \tau_{\text{fac}}$ and U. By inspection of these diagrams and Fig. 5B, one observes that the width of the oscillatory phase enlarges for increasing values of τ_{fac} and decreases with T.

A detailed analysis of the oscillatory phase shows that the access to the stored memories and the error in the retrieval of such memories strongly depends on facilitation and on its competition with depression. This is shown in Fig. 6 where the half period of the oscillations in the overlap with a pattern $m \equiv m_+ - m_-$ and its maximum absolute

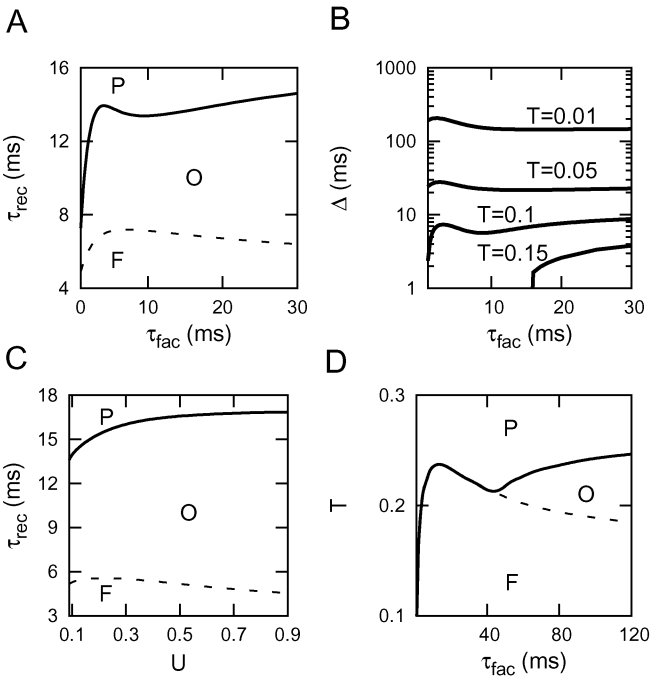

FIGURE 5. Phase diagrams for $\alpha = 0$ and several values of the relevant parameters defining the dynamics of the synapses, namely $U, \tau_{\rm rec}, \tau_{\rm fac}$ and T. The panel A represents the phase diagram in the plane $(\tau_{\rm rec}, \tau_{\rm fac})$ at temperature $T = 0.1$ and $U = 0.1$. The dashed (solid) line correspond to the line of critical $\tau^*_{\rm rec}$ ($\tau^{**}_{\rm rec}$) where recall (oscillatory) phase disappears. In the panel B it is shown, from top to bottom, the width of the oscillatory phase, defined as $\Delta = \tau^{**}_{\rm rec} - \tau^*_{\rm rec}$, in the $(\tau_{\rm rec}, \tau_{\rm fac})$ plane for increasing values of the temperature. Panel C corresponds to the phase diagram in the plane $(\tau_{\rm rec}, U)$ for $T = 0.1$ and $\gamma \equiv \tau_{\rm fac}/\tau_{\rm rec} = 0.25$. Panel D is the phase diagram in the plane $(T, \tau_{\rm fac})$ for $U = 0.1$ and $\tau_{\rm rec} = 3$ ms. In panels A,C and D, solid lines correspond to second order phase transitions and dashed lines to first-order phase transitions.

value is represented as function of $\tau_{\rm fac}$, for different values of $\tau_{\rm rec}$ and $U = T = 0.1$. The appearance of the oscillatory phase is the result of the instability of the fixed-point ferromagnetic solutions, as in the model of the previous section. However, in this case dynamics is periodic for the case of one pattern.

We have also investigated, for several values of the depressing and facilitating parameters and in the limit of $\alpha \to 0$ $(M = 1)$, the sensitivity of the network under external stimulation, namely $I_i^{\rm ext} = \pm\delta\xi_i^1$, during a time interval of 20 ms. The pulse is such that it takes a positive value at time t if $m^1(t-1) < 0$ and a negative value if $m^1(t-1) > 0$. Some of the resulting picture is illustrated in Fig. 7, where the network is responding to a periodic external stimulus of amplitude $\delta = 0, 0.01, 0.1, 0.4$. This shows (left panels) how the presence of an activity-dependent dynamics on the synapses through the variable $r(t)$ induces instability of the memories, which allows for a better response to the

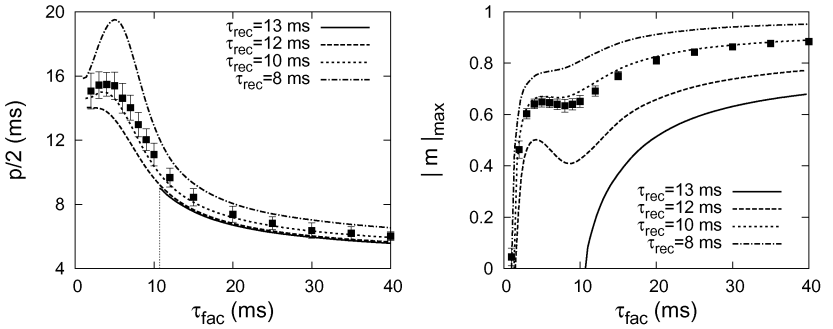

FIGURE 6. (Left) Dependence of the half period during the oscillatory regime as a function of $\tau_{\rm fac}$. (Right) Dependence of the maximum of the overlap m as a function also of $\tau_{\rm fac}$ and four different values of $\tau_{\rm rec}$. Both panels illustrate that strong facilitation (large values of $\tau_{\rm fac}$) produces a more rapid access to stored information and with less error, in particular when depression is not so high (smaller values of $\tau_{\rm rec}$). The figure also shows the opposite effect due to depression, that appear for week facilitation (small values of $\tau_{\rm fac}$). Data points correspond to Monte Carlo simulations for $\tau_{\rm rec} = 10$ ms confirming the mean field results. The vertical dashed line in the left panel marks the critical value of $\tau_{\rm fac}$ in which the oscillations disappear for $\tau_{\rm rec} = 13$ ms.

stimulus even if it is very week. On the contrary, for static synapses as in the Hopfield model (right panels), the system is not sensible to stimulus and only when its amplitude is very large some tiny level of response appears in the network activity. The figure also shows that increasing facilitation, that is for larger values of $\tau_{\rm fac}$, the stability of the ferromagnetic solution also increases. This is shown in the second left panel of the figure where increasing $\tau_{\rm fac}$ from 0 to 80 ms impedes a efficient response to a week stimulus of $\delta = 0.01$.

The case of many stored memories, can still be studied numerically. Preliminary studies show that, similarly to the case of only one pattern, there are three main phases. That is, paramagnetic, ferromagnetic and complex oscillatory phases where, depending on the relevant parameters, the activity jumps between memory and mixture states. An example of this behavior is shown in Fig. 8. The figure represents the autonomous behavior of the network activity in the oscillatory phase for $\tau_{\rm rec} = 40$ ms, $T = 0.01$, $U = 0.1$ and $M = 10$ overlapping patterns, each one with M consecutive neurons in an active state, namely $\xi_i^\nu = 1$, starting at positions $1 + \nu N/M$, with $\nu = 0 \ldots M-1$. The top and bottom raster plots correspond, respectively, to $\tau_{\rm fac} = 10$ and 200 ms. This figure shows how an increase of the facilitation effect allows for a faster access to stored information but during a shorter period of time

We have also investigated the response of the network under external stimuli when it stores many patterns ($\alpha \neq 0$). An example of this study is showed in Fig. 9. The figure shows (left panels) that including realistic dynamic synapses responds more efficient to a varying external stimulus, even when the stimulus is very week (Note that the amplitude of the stimulus is $\delta = 0.1$ in this simulation). On the contrary, the static Hopfield network is unable to respond to the stimulus. Only when its amplitude becomes large enough

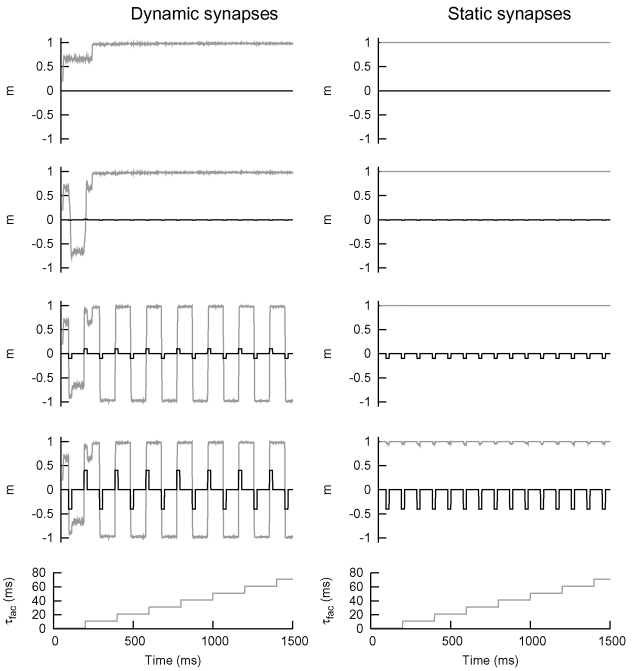

FIGURE 7. Response of the network activity, measured in terms of the overlap m, under a periodic external stimulus for dynamic (left panels) and static (right panels) synapses in the limit $\alpha \to 0$ ($M = 1$). Simulation parameters are $T = 0.1, U = 0.1, \tau_{\rm rec} = 3$ ms for dynamic synapses and $T = 0.1, U = 1, \tau_{\rm rec} = 0$ ms for static synapses. The increasing $\tau_{\rm fac}$ protocol from $\tau_{\rm fac} = 0$ ms to $\tau_{\rm fac} = 80$ ms plotted in the two bottom graphs was applied in both cases. In the case of static synapses this protocol has no effect because $U = 1$.

($\delta = 0.42$) the system begins to have some non-efficient response to the stimulus (See right panels). These results agree quantitative and qualitatively with those reported in the previous section for the fast-noise depression model.

DISCUSSION

We have reviewed here a theoretical framework to study different models of activity-dependent processes which occur at different time scales in neural networks. We have first introduced a model which includes biologically motivated synaptic noise whose dynamics is coupled with that of the network activity via the steady-state noise distribution (5). This aims to mimic synaptic depression and/or facilitation. It follows that the network exhibits much more varied and intriguing behavior than the standard static Hopfield model. For instance, the network exhibits for $\Phi < 1$ a high sensitivity to external stimuli and, in some conditions, chaotic jumping among the stored memories, which

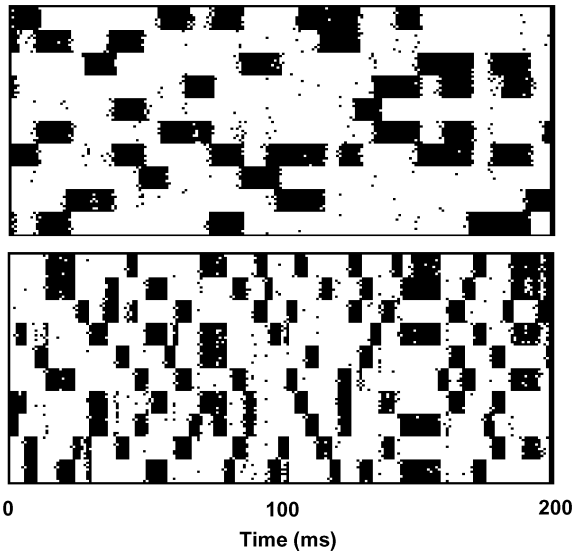

FIGURE 8. Raster plots showing the behaviour of $N = 100$ binary neurons with dynamic synapses including facilitating mechanisms. Each black dot corresponds to a neuron firing event. Top and bottom graphs correspond to $\tau_{\text{fac}} = 10$ ms and 200 ms, respectively. Other parameters are $\tau_{\text{rec}} = 40$ ms, $T = 0.01$, $U = 0.1$ and $M = 10$ overlapping patterns.

allows for better exploring the stored information. The theoretical framework presented is general enough to allow for investigating more realistic assumptions concerning the noise distribution; in this way, the presented models can be related to other models in the literature.

On the other hand, we have illustrated that networks including phenomenologically-motivated dynamical synapses which account for short-term facilitation and depression show complex behavior which depends on the relative balance between depression and facilitation. For low depression, a memory phase occurs. For very large depression or facilitation, the phase exhibits no memory. For intermediate facilitation and/or depression, an oscillatory phase with the activity of the network jumping between the attractors appears. We also observed that a high facilitation enhances the network ability to switch among the stored patterns, as well as its adaptation to external stimuli [15]. Other interesting new phenomena are, for instance, that the memory phase disappears earlier for a fixed degree of depression and temperature. Moreover, we observe in the oscillatory phase that its width in the corresponding phase diagram increases with facilitation, as shown in Fig. 5. In addition, the frequency of the oscillations also increases with facilitation. As a consequence, it seems one should conclude that facilitation allows to recover stored information with less error but during a shorter period of time. This supports the idea that synaptic facilitation influences the processes of short-term memory. The facility to switch could be interesting to code both spatial and temporal information, and could explain, for instance, the spatio-temporal dynamics in the early olfactory processes [16].

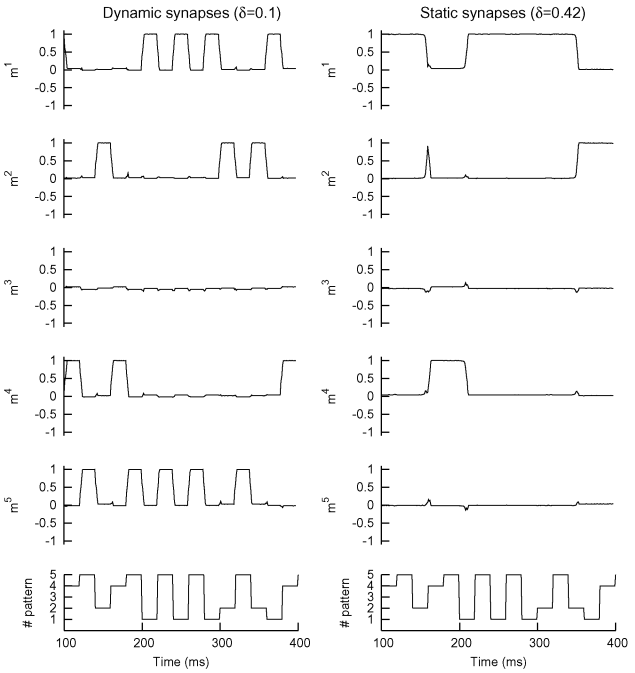

FIGURE 9. Response of a neural network of $N = 1000$ neurons storing $M = 5$ random patterns under a time varying external stimulus $I_i^{\text{ext}} = \delta \xi_i^{\nu}$, where ν changes randomly during time in the set $[1, M]$ (see two bottom panels). Left panels shows that the response of the network to stimuli is efficient for dynamic synapses even for very small stimulus amplitude ($\delta = 0.1$). On the contrary right panels show a non-efficient response for static synapses even for very large stimulus amplitude ($\delta = 0.42$). The two bottom panels show the pattern that every time is presented to the network in the stimulus.

ACKNOWLEDGMENTS

This work was supported by the MEyC-FEDER project FIS2005-00791 and the Junta de Andalucía project FQM-165. JMC also acknowledges financial support from EPSRC-funded COLAMN project Ref. EP/CO 10841/1. We thank useful discussion with Jorge F. Mejías.

REFERENCES

1. L. F. Abbott, and W. G. Regehr, *Nature* **431**, 796–803 (2004).
2. D. J. Amit, *Modeling brain function: the world of attractor neural network*, Cambridge University Press, 1989.
3. P. Peretto, *An Introduction to the modeling of neural networks*, Cambridge University Press, 1992.
4. C. Allen, and C. F. Stevens, *Proc. Natl. Acad. Sci. USA* **91**, 10380–10383 (1994).

5. A. Zador, *J. Neurophysiol.* **79**, 1219–1229 (1998).
6. K. M. Franks, C. F. Stevens, and T. J. Sejnowski, *J. Neurosci.* **23**, 3186–3195 (2003).
7. M. V. Tsodyks, K. Pawelzik, and H. Markram, *Neural Comp.* **10**, 821–835 (1998).
8. A. M. Thomson, A. P. Bannister, A. Mercer, and O. T. Morris, *Philos. Trans. R. Soc. Lond. B Biol. Sci.* **357**, 1781–1791 (2002).
9. Note: Our restriction to binary neurons is not expected to influence essentially our results. In fact, it has been shown, for instance, that the behavior of binary networks agrees qualitatively with the behavior observed in more realistic networks of integrate and fire neuron models [10].
10. L. Pantic, J. J. Torres, H. J. Kappen, and S. C. A. M. Gielen, *Neural Comp.* **14**, 2903–2923 (2002).
11. J. J. Torres, P. L. Garrido, and J. Marro, *J. Phys. A: Math. Gen.* **30**, 7801–7816 (1997).
12. J. Marro, and R. Dickman, *Nonequilibrium Phase Transitions in Lattice Models*, Cambridge University Press, 1999.
13. J. M. Cortes, J. Torres, J. Marro, P. Garrido, and H. Kappen, *Neural Comp.* **18**, 614–633 (2006).
14. J. Marro, J. J. Torres, J. M. Cortes, and B. Wemmenhove, cond-mat/0604662 (2006).
15. J. J. Torres, J. Cortes, J. Marro, and H. Kappen, *Neural Comp.* (2006), in press.
16. G. Laurent, M. Stopfer, R. W. Friedrich, M. I. Rabinovich, A. Volkovskii, and H. D. I. Abarbanel, *Annu. Rev. Neurosci.* **24**, 263–297 (2001).